

Charged pion-pair photoproduction and electroproduction on the proton up to 1 GeV

Saro Ong and Jacques Van de Wiele

Institut de Physique Nucléaire, IN2P3-CNRS, Université Paris-Sud, F-91406 Orsay Cedex, France

(Received 29 June 2000; published 24 January 2001)

An effective Lagrangian approach for double pion photoproduction and electroproduction on the proton developed by the Valencia group is improved in a covariant relativistic way. We obtain reasonable agreement with available experimental data for charged pion-pair channel from threshold up to 1 GeV. The role of the $D_{13}(1520)$ resonance in this channel as an intermediate state is also discussed. This approach is applied to calculate the π^- inclusive cross section.

DOI: 10.1103/PhysRevC.63.024614

PACS number(s): 25.20.Lj, 13.60.Le, 13.60.Rj

I. INTRODUCTION

The $\gamma p \rightarrow \pi^+ \pi^- p$ reaction was investigated first in Ref. [1] using five Feynman diagrams in the framework of the gauge-invariant extended one-pion exchange mechanism. They obtain reasonable agreement with experimental data from the Aachen-Berlin-Bonn-Hamburg-Heidelberg-Munich Collaboration [2].

All possible double pion photoproduction reactions on the nucleon have been studied by the Valencia group [3] using effective Lagrangian and incorporating a set of resonances $\Delta(1232)$, $P_{11}(1440)$, and $D_{13}(1520)$. These predictions have been found to be consistent with all available data [2,4,5]. Some discrepancies remain in $\gamma p \rightarrow \pi^+ \pi^0 n$ and $\gamma n \rightarrow \pi^- \pi^0 p$ channels, recently measured [6]. The role of the D_{13} -resonance and in particular its interference with the dominant components of the process (Kroll-Ruderman [7] and pion-pole terms) is emphasized. In addition to single pion photoproduction, where the D_{13} plays an essential role in the second resonance region, the double pion channel allows one to investigate the relative phase of this resonance to those of different amplitudes involved through interference terms.

The predictions of the authors of Ref. [8] are compatible with the invariant mass spectra measured for the $(p \pi^\pm)$ systems from the $\gamma p \rightarrow \pi^+ \pi^- p$ reaction, both on hydrogen and deuterium [6].

A recent dynamical model for the resonances $\Delta(1232)$, $D_{13}(1520)$ and the ρ meson [9] can reproduce the $\gamma p \rightarrow \pi^+ \pi^0 n$ data. However, a finite range form factor was given to the $\rho \pi \pi$ vertex.

Another interesting $\gamma p \rightarrow \pi^0 \pi^0 p$ reaction close to threshold has been used to test the heavy baryon chiral perturbation theory [10]. The main result of this investigation is the enhancement of the production cross section due to chiral (pion) loop corrections.

The precise measurements performed or planned at Mainz with the large acceptance detector Daphne [5,6], at ESRF with Graal [11], and at TJNAF would clarify the role of these resonances and the chiral loop corrections near threshold in double neutral pion production channels.

In the present study, we reexamine the charged pion-pair photoproduction and electroproduction on the proton which is largely investigated by the Valencia group [3,12,13]. Following our previous study on single pion photoproduction

and electroproduction [14], we suggest a covariant relativistic approach to this problem, rewriting the coupling of photons and pions to nucleons and resonances using effective Lagrangians, and we derive the Feynman rules for the different diagrams at the tree level. The spinors of the nucleon and the resonances (Δ and D_{13}) are treated in a covariant relativistic way; this is not the case in [12]. The Δ resonance is considered as an intermediate state in the various Feynman diagrams involved. This means that the Δ is treated as a propagator and for the spin 3/2 particle, we adopt the prescription of Rarita-Schwinger [15], whereas the approach in Ref. [12] uses the nonrelativistic propagator of the nucleon and Δ resonance.

The large coupling of the $D_{13}(1520)$ to the photon and the gauge invariance of the electromagnetic current in the present paper are largely inspired from the previous work of Garcilazo *et al.* [16].

This study has been also developed for the parity violating elastic electron-proton scattering experiment G0, in the backward scattering configuration planned at TJNAF [17], with an electron beam energy in the range of 0.335–0.940 GeV. Effectively, a π^- coming from double pion electroproduction channel can simulate a scattered electron; such processes in principle could introduce important background. In this study, the Δ is not considered as a final state, this allows one to control the angular distribution of the pions coming from $\Delta \rightarrow \pi N$ decays.

The π^- inclusive cross section is evaluated without a zero electron mass approximation and the polarized electron vertex is considered in an exact way.

Our paper is organized as follows. In Sec. II we develop a model for double pion photoproduction and electroproduction from threshold up to 1 GeV. Comparison is made with available experimental data to check the consistency of our analysis. In Sec. III, we estimate double pion electroproduction contribution in the kinematical configuration of G0 experiment. We summarize the main result of our analysis in Sec. IV.

II. MODEL OF DOUBLE PION PHOTOPRODUCTION AND ELECTROPRODUCTION

We reexamine the reaction $\gamma p \rightarrow \pi^+ \pi^- p$ in order to check the consistency of our analysis. For this channel, we do not implement unitarity in the final states and we assume

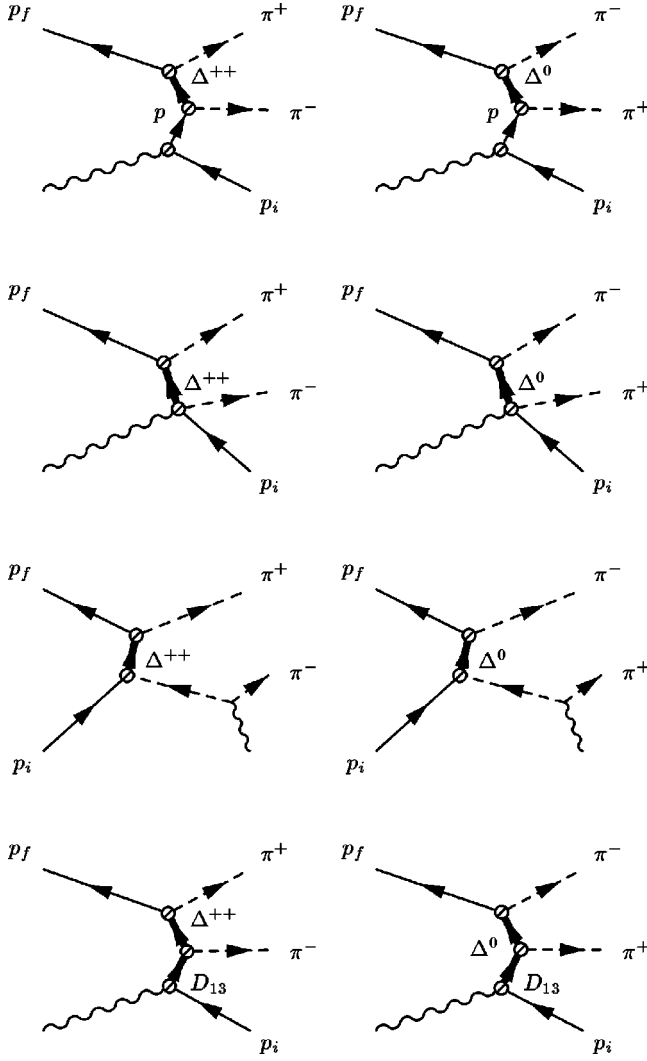


FIG. 1. Feynman diagrams of the main contributions for $\gamma p \rightarrow \pi^+ \pi^- p$ which have a Δ in the intermediate state.

that the contribution of the diagrams containing a $\rho\pi\pi$ vertex is negligible at these energies. However, in order to reproduce the invariant mass spectra [6] for the $(\pi^- \pi^0)$ system at higher photon energies in the $\gamma n \rightarrow \pi^- \pi^0 p$ reaction, the authors of Ref. [9] predict an important role of the intermediate excitation ρN state, assuming a finite range form factor to the $\rho\pi\pi$ vertex.

In the energy range in which we are interested, from threshold up to 1 GeV, the effective Lagrangian model should be applied in detail with good accuracy. Expressions of the interaction Lagrangians are displayed in Appendix A. In Appendix B, we derive the corresponding Feynman rules at each vertex of the diagrams shown in Figs. 1 and 2 required in the reaction of our interest. The main contribution comes from the diagrams in Fig. 1, in particular the Kroll-Ruderman and the pion pole terms. Let us notice the important role of the D_{13} resonance which interferes with the dominant term, allowing one to get information about the sign of the s and d wave amplitudes of $D_{13} \rightarrow \Delta N$. The set of diagrams in Fig. 2 is needed to preserve gauge invariance

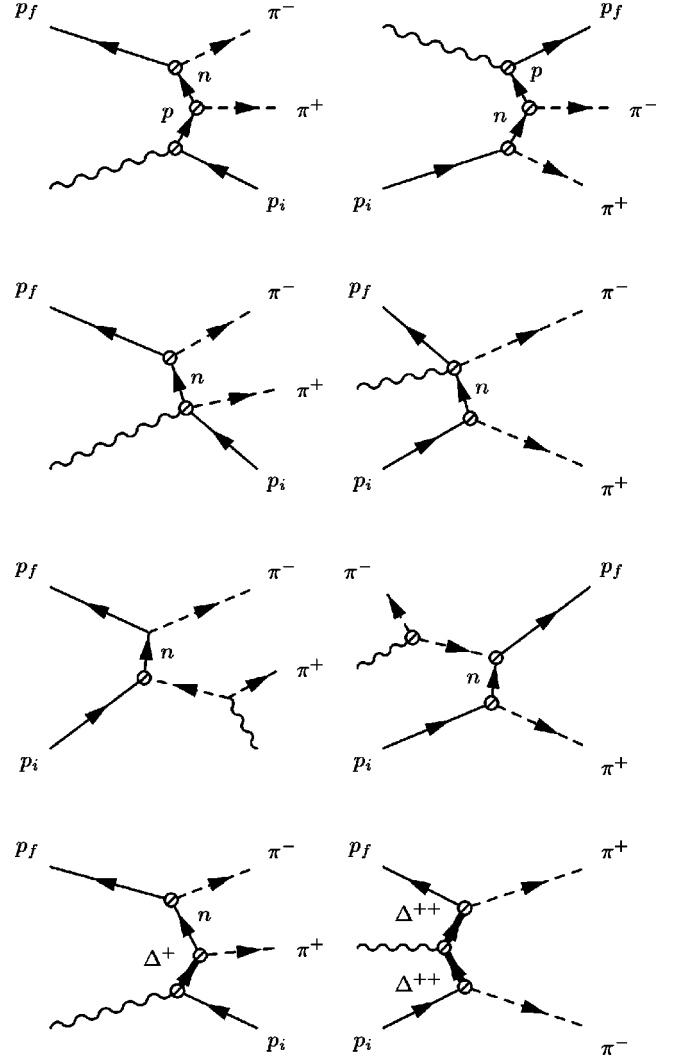


FIG. 2. The set of other Feynman diagrams for $\gamma p \rightarrow \pi^+ \pi^- p$ included in our model (see text).

and also to reproduce the data, in particular near the threshold (Fig. 3).

The amplitude calculations of double pion photoproduction has been performed by numerically evaluating the matrix elements. We emphasize the agreement between the different Lagrangian terms used in this study and those in the previous paper on one pion electroproduction [14].

The cross section for the $\gamma p \rightarrow \pi^+ \pi^- p$ is given by a differential form with respect to the outgoing pions:

$$\frac{d^5 \sigma^\gamma}{dE_{\pi^-}^* d\Omega_{\pi^-}^* d\Omega_{\pi^+}^*} = \frac{1}{(2\pi)^5} \frac{1}{32W} \frac{|\vec{p}_{\pi^-}^*|}{E_\gamma^*} \frac{|\vec{p}_{\pi^+}^*|^3}{|\vec{p}_{\pi^+}^{*2} E_p^* + E_{\pi^+}^* (\vec{p}_{\pi^+}^{*2} + \vec{p}_{\pi^+}^* \cdot \vec{p}_{\pi^-}^*)|} \times \langle |\mathcal{M}|^2 \rangle. \quad (1)$$

The different variables in Eq. (1) are expressed in the cm frame of the photon-target proton. W is the photon-proton

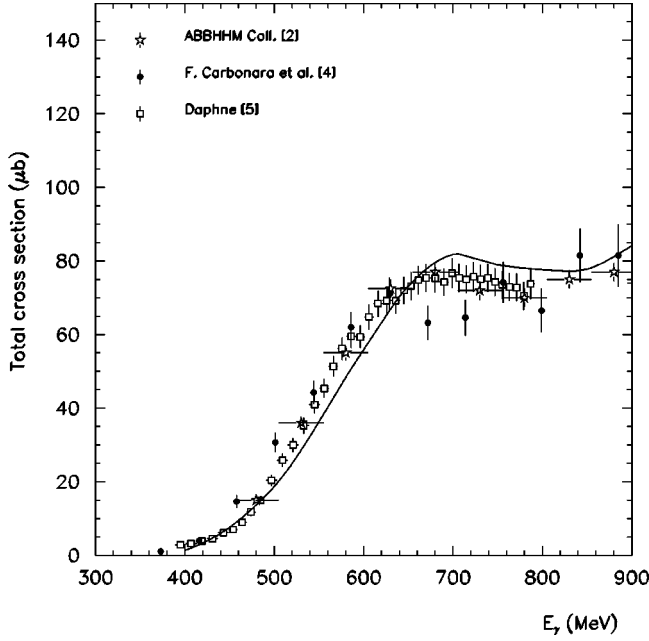


FIG. 3. Total cross section prediction for $\gamma p \rightarrow \pi^+ \pi^- p$ as a function of the real photon energy.

center of mass energy, E_p^* is the energy of the recoil proton and $\langle |\mathcal{M}|^2 \rangle$ is the mean value of the absolute square of the invariant matrix element for $\gamma p \rightarrow \pi^+ \pi^- p$, taking into account all helicity states of ingoing and outgoing particles.

For the construction of electromagnetic currents for resonance excitation in double pion electroproduction, appropriate form factors must be considered to preserve the gauge invariance. To implement the Q^2 dependence, the Lagrangian terms (A7) and (A10), given in Appendix A, should contain a third term with an additive form factor G_3 . For example, the term (A7) is replaced by

$$\begin{aligned} \mathcal{L}_{\gamma ND_{13}} = & -\frac{G_1}{4M} \bar{\Psi}_{D_{13}}^p (g_{\rho\mu} \gamma_\nu - g_{\rho\nu} \gamma_\mu) \{ \vec{\tau}, 1 \} \Psi_N F^{\mu\nu} \\ & + \frac{G_2}{8M^2} \bar{\Psi}_{D_{13}}^p (g_{\rho\nu} P_\mu - g_{\rho\mu} P_\nu) \{ \vec{\tau}, 1 \} \Psi_N F^{\mu\nu} \\ & + \frac{G_3}{4M^2} \bar{\Psi}_{D_{13}}^p i (g_{\rho\mu} g_{\nu\mu} \partial_\mu F^{\mu\nu} - g_{\rho\nu} g_{\mu\nu} \partial_\nu F^{\mu\nu}) \\ & \times \{ \vec{\tau}, 1 \} \Psi_N + \text{H.c.} \end{aligned} \quad (2)$$

The parametrizations of these form factors are investigated in Refs. [12,18,19]. In the kinematical region where ($Q^2 \sim 0$), one can neglect the term containing G_3 . We adopt this strategy to suppress another free parameter introduced by G_3 in our analysis.

We assume the dipole type for the electric form factor:

$$G_E^p = \left(1 + \frac{Q^2}{\Lambda^2} \right)^{-2}, \quad (3)$$

with $\Lambda^2 = 0.71 \text{ GeV}^2$.

The expressions of $F_1^p(Q^2)$ and $F_2^p(Q^2)$ are given in the following form:

$$F_1^p(Q^2) = \frac{G_E^p + \tau G_M^p}{1 + \tau}, \quad (4)$$

$$F_2^p(Q^2) = \frac{G_M^p - G_E^p}{1 + \tau}, \quad (5)$$

with $\tau = Q^2/4M_p^2$, $G_M^p = \mu_p G_E^p$ ($\mu_p = 2.793$).

The Q^2 dependence of G_1 and G_2 is taken in the simple monopole type:

$$G_1(Q^2) = G_1(0) \frac{1}{\left(1 + \frac{Q^2}{\Lambda^2} \right)}, \quad (6)$$

$$G_2(Q^2) = G_2(0) \frac{1}{\left(1 + \frac{Q^2}{\Lambda^2} \right)}. \quad (7)$$

For the delta resonance, we follow the prescriptions of the authors of Ref. [12]

$$F_1^\Delta(Q^2) = F_1^p(Q^2), \quad (8)$$

$$G_M^\Delta(Q^2) = \mu_\Delta G_E^p(Q^2). \quad (9)$$

In the case of Δ^{++} , we use the experimental value $\mu_\Delta = 1.62\mu_p$.

For the pion-pole diagram in Fig. 1, the exchanged pion is off-shell and we use a form factor of the monopole type:

$$F_\pi(p^2) = \frac{\Lambda_\pi^2 - m_\pi^2}{\Lambda_\pi^2 - p^2},$$

with $\Lambda_\pi = 900 \text{ MeV}$. The Kroll-Ruderman and the $(p-\Delta)$ diagrams in Fig. 1 are affected by the same factor which is motivated to preserve gauge invariance.

The contributions of each vertex in Appendix B are now well defined and one can write down the differential cross section for the double pion electroproduction as being

$$\frac{d^8\sigma}{dE_e' d\Omega_e dE_{\pi^-}^* d\Omega_{\pi^-}^* d\Omega_{\pi^+}^*} = \Gamma \frac{d^5\sigma^\gamma}{dE_{\pi^-}^* d\Omega_{\pi^-}^* d\Omega_{\pi^+}^*}, \quad (10)$$

where $d^5\sigma^\gamma/dE_{\pi^-}^* d\Omega_{\pi^-}^* d\Omega_{\pi^+}^*$ is the virtual photoproduction cross section of the process $\gamma^* p \rightarrow p \pi^+ \pi^-$ and Γ is a known flux factor given by

$$\Gamma = \frac{\alpha}{2\pi^2} \frac{E_e'}{E_e} \frac{E_\gamma}{Q^2} \frac{1}{1-\varepsilon} \quad (11)$$

in the limit $m_e = 0$. $Q^2 = -q^2 = 2E_e E_e' (1 - \cos \theta_e)$ and $W^2 = M^2 - Q^2 + 2M(E_e - E_e')$, where E_e and E_e' are the laboratory energies of the incident and scattered electron and M is

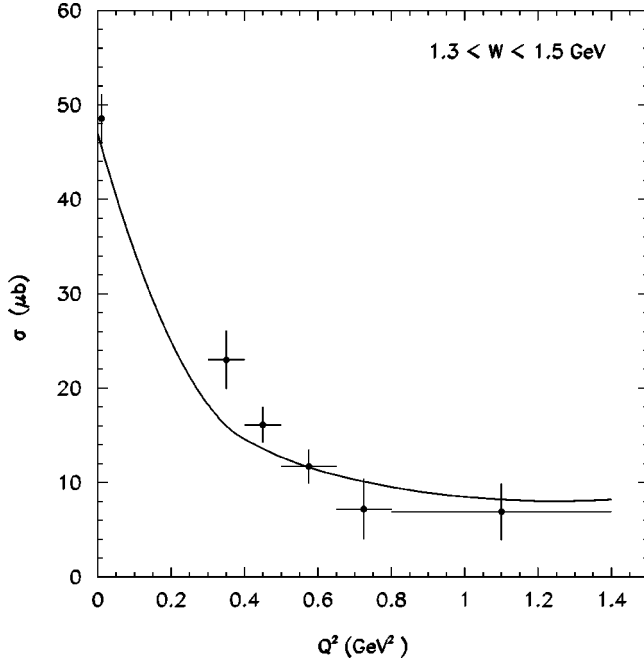


FIG. 4. Cross section of $\gamma_0 p \rightarrow \pi^+ \pi^- p$ as a function of Q^2 .

the mass of the proton. $E_\gamma = (W^2 - M^2)/2M$ is the laboratory energy necessary for a real photon to excite the hadronic system with mass M to the cm energy W , and the quantity $\varepsilon = (1 + 2|\vec{q}|^2 \tan^2(\theta_e/2)/Q^2)^{-1}$ characterizes the transverse polarization of the virtual photon.

One can integrate Eq. (10) over the pion variables and rewrite the differential cross section for electroproduction with the invariant quantities Q^2 and W , in the following form:

$$\frac{d^2\sigma}{dQ^2 dW} = \frac{\pi W}{ME_e E'_e} \Gamma[\sigma_T(Q^2, W) + \varepsilon \sigma_L(Q^2, W)]. \quad (12)$$

$\sigma_T(Q^2, W)$ and $\sigma_L(Q^2, W)$ are the proton absorption cross sections for transverse and longitudinal polarized virtual photons respectively. In this form, a comparison can be made with available data [20] on the double pion electroproduction reaction with $0.3 < Q^2 < 1.4 \text{ GeV}^2$ and a range of $1.3 < W < 1.5 \text{ GeV}$ (Fig. 4). We have averaged the cross section values calculated between $1.3 < W < 1.5 \text{ GeV}$. The data point at $Q^2 = 0$ in Fig. 4 is obtained by averaging the experimental data [5]. The agreement with the data is very good. For higher values of W ($W > 1.5 \text{ GeV}$), our model cannot accommodate the data; the ρ^0 -production channel is found to be important [20]. This shows the validity domain of this model, which is the same as in the photoproduction channel (Fig. 3).

It can be seen that a reasonable agreement with the data is obtained with our model for different kinematical regions both in double pion photo and electroproduction. We are going to discuss, in the next section, the π^- contamination in backward scattering configuration of G0 experiment.

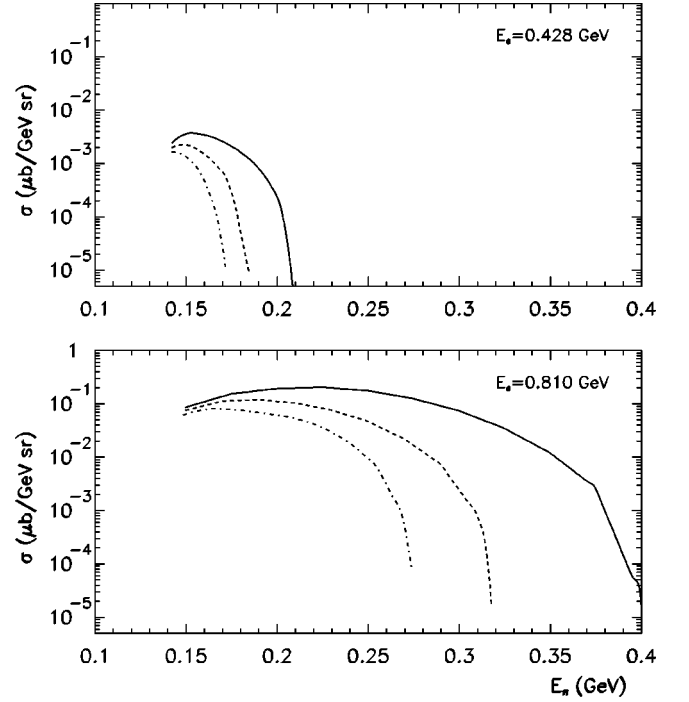


FIG. 5. Differential cross section $d^2\sigma/dE_{\pi^-} d\Omega_{\pi^-}$ for $ep \rightarrow ep \pi^+ \pi^-$ versus the π^- laboratory energy, and for two values of the electron beam energy (428 and 810 MeV). Solid line: $\theta_{\pi} = 60^\circ$; dashed line: $\theta_{\pi} = 100^\circ$; and dash-dotted line: $\theta_{\pi} = 140^\circ$.

III. PION CONTAMINATION IN ELASTIC ep SCATTERING

We investigate the double pion electroproduction channel as an important background source for the G0 experiment which is planned at TJNAF to measure parity violating asymmetry in elastic ep scattering. In this experiment, the parity-violating asymmetry will be measured at forward and backward angles in order to perform the precise Rosenbluth separation of G_E^Z and G_M^Z , the neutral weak electric and magnetic form factors of the proton. The strange quark form factors $G_{E,M}^s$ can be related to the $G_{E,M}^Z$ and the electromagnetic form factors of the nucleon $G_{E,M}^{p,n}$:

$$G_{E,M}^Z = \left(\frac{1}{4} - \sin^2 \theta_W \right) G_{E,M}^p - \frac{1}{4} G_{E,M}^n - \frac{1}{4} G_{E,M}^s. \quad (13)$$

The forward angle asymmetries in different Q^2 bins from 0.2 to 1.0 GeV^2 will be measured simultaneously utilizing a beam energy of 3.2 GeV.

The backward configuration measurements for each Q^2 point will require a different beam energy in the range of 0.335–0.940 GeV. Only the scattered electrons are detected at $\theta_e = 108^\circ$. The π^- contamination coming from double pion electroproduction channel is important for extracting the tiny asymmetry term with high accuracy. We have shown in the previous section that our model can offer valuable predictions for this channel in this range of energy.

For an accurate estimation of this contamination, we need to calculate the cross section

$$\begin{aligned} & \frac{d^3\sigma}{dE_{\pi^-} d\Omega_{\pi^-}} \\ &= \int \frac{d^8\sigma}{dE'_e d\Omega_e dE_{\pi^-} d\Omega_{\pi^-} d\Omega_{\pi^+}^R} dE'_e d\Omega_e d\Omega_{\pi^+}^R, \end{aligned} \quad (14)$$

where E_{π^-} and Ω_{π^-} are the laboratory frame variables of the π^- , while the $\Omega_{\pi^+}^R$ is the solid angle of the π^+ in the (π^+ -proton) center-of-mass frame:

$$\begin{aligned} & \frac{d^8\sigma}{dE'_e d\Omega_e dE_{\pi^-} d\Omega_{\pi^-} d\Omega_{\pi^+}^R} \\ &= \frac{1}{(2\pi)^8} \frac{1}{64M|\vec{p}_e|} \frac{|\vec{p}_e'| |\vec{p}_{\pi^-}| |\vec{p}_{\pi^+}^R|}{W_R} \langle |\mathcal{M}|^2 \rangle. \end{aligned} \quad (15)$$

W_R is the (π^+ -proton) center of mass energy, $\vec{p}_{\pi^+}^R$ is the

momentum of the π^+ in the same frame. \vec{p}_e , \vec{p}_e' and \vec{p}_{π^-} are the momenta of the incident electron, scattered electron, and the π^- in the laboratory frame, respectively.

We display in Fig. 5 the E_{π^-} dependence of the differential cross section for $ep \rightarrow ep \pi^+ \pi^-$ at different values of θ_{π^-} . Two values of the electron beam energy are selected, corresponding to Q^2 values of 0.3 and 0.8 GeV².

Special attention to very small Q^2 values permitting an exact consideration of effects with nonzero electron mass is very important here, given that the main contribution to the photon spectrum is due to $Q^2 \simeq 0$.

We emphasize the important effect of the electron mass ($m_e \neq 0$) in the integral calculation of Eq. (14). The factorization formula (10) can be used to estimate this cross section with caution. The popular virtual photon spectrum concept [21] is useful to extract the electron induced cross section from the photon induced cross section.

In this study, the virtual photon spectrum concept is extended to the case of a polarized electron beam. Formula (10) should then be rewritten allowing for an incident electron helicity h , a scattered electron helicity h' and the helicities of the nucleon target and recoil nucleon h_N , h'_N , respectively,

$$\frac{d^8\sigma_h}{dE'_e d\Omega_e dE_{\pi^-}^* d\Omega_{\pi^-}^* d\Omega_{\pi^+}^*} = \frac{1}{128(2\pi)^8} \frac{|\vec{p}_e'| |\vec{p}_{\pi^-}^*|}{|\vec{p}_e| M} \frac{|\vec{p}_{\pi^+}^*|^3 |\mathcal{M}|^2}{|\vec{p}_{\pi^+}^{*2} E_p^* + E_{\pi^+}^* (\vec{p}_{\pi^+}^{*2} + \vec{p}_{\pi^+}^* \cdot \vec{p}_{\pi^-}^*)|}, \quad (16)$$

with

$$\begin{aligned} |\mathcal{M}|^2 = & O_{-1,-1} \sum_{h'} |A_{[-1]}(h, h')|^2 + O_{1,1} \sum_{h'} |A_{[1]}(h, h')|^2 + 2 \operatorname{Re} \left[O_{-1,1} \sum_{h'} A_{[-1]}(h, h') A_{[1]}^*(h, h') \right] \\ & + 2 \operatorname{Re} \left[O_{-1,0} \sum_{h'} A_{[-1]}(h, h') A_{[0]}^*(h, h') \right] + 2 \operatorname{Re} \left[O_{0,1} \sum_{h'} A_{[0]}(h, h') A_{[1]}^*(h, h') \right] + O_{0,0} \sum_{h'} |A_{[0]}(h, h')|^2. \end{aligned} \quad (17)$$

In the γ^*p c.m. frame the virtual photon polarization vector $\varepsilon_{[\lambda]}^\mu$ reads as

$$\varepsilon_{[0]} = \frac{1}{Q} (|\vec{q}^*|, 0, 0, q_0^*), \quad \varepsilon_{[\pm]} = \frac{1}{\sqrt{2}} (0, \mp 1, -i, 0). \quad (18)$$

The hadronic tensor $O_{\lambda, \lambda'}$, calling $\lambda, \lambda' = 0, \pm 1$ the helicities of γ , is expressed in terms of the hadron current matrix element $J_\mu(h_N, h'_N)$ in the following form:

$$O_{\lambda, \lambda'} = \sum_{\mu, \nu} \sum_{h_N, h'_N} \varepsilon_{[\lambda]}^\mu \varepsilon_{[\lambda']}^{*\nu} J_\mu(h_N, h'_N) J_\nu^*(h_N, h'_N). \quad (19)$$

Let us remark that the Hermiticity relation $O_{\lambda', \lambda} = O_{\lambda, \lambda'}^*$, entails formula (17).

In the limit $Q^2 \rightarrow 0$ and with an unpolarized electron beam, the formula (16) is reduced to a factorization form

$$\frac{d^8\sigma}{dE'_e d\Omega_e dE_{\pi^-}^* d\Omega_{\pi^-}^* d\Omega_{\pi^+}^*} = \bar{\Gamma} \frac{d^5\sigma^\gamma}{dE_{\pi^-}^* d\Omega_{\pi^-}^* d\Omega_{\pi^+}^*}, \quad (20)$$

where the flux factor reads as

$$\bar{\Gamma} = \frac{\alpha}{8\pi^2} \frac{|\vec{p}_e'|}{|\vec{p}_e|} E_\gamma F_{virt} \quad (21)$$

and

$$F_{virt} = \sum_{h, h'} [|A_{[1]}(h, h')|^2 + |A_{[-1]}(h, h')|^2], \quad (22)$$

$$F_{virt} = \frac{2}{Q^4 |\vec{q}|^2} (X_1 + X_2 + X_3), \quad (23)$$

$$-Q^2 = q^2 = 2[m_e^2 - (E_e E_e' - |\vec{p}_e| |\vec{p}_e'| \cos\theta_e)], \quad (24)$$

$$|\vec{q}|^2 = (|\vec{p}_e| - |\vec{p}'_e|)^2 + 4|\vec{p}_e||\vec{p}'_e|\sin^2(\theta_e/2), \quad (25)$$

$$X_1 = [|\vec{q}|^2 + \mathcal{Y}^2][\mathcal{A}_1^2 \sin^2(\theta_e/2) + \mathcal{B}_1^2 \cos^2(\theta_e/2)], \quad (26)$$

$$X_2 = 4|\vec{p}'_e|^2 \sin^2(\theta_e/2) \cos^2(\theta_e/2) \\ \times [\mathcal{A}_1^2 \cos^2(\theta_e/2) + \mathcal{B}_1^2 \sin^2(\theta_e/2)], \quad (27)$$

$$X_3 = 4\mathcal{Y}|\vec{p}'_e|\sin^2(\theta_e/2)\cos^2(\theta_e/2)[\mathcal{A}_1^2 - \mathcal{B}_1^2], \quad (28)$$

$$\mathcal{Y} = |\vec{p}_e| - |\vec{p}'_e| + 2|\vec{p}'_e|\sin^2(\theta_e/2), \quad (29)$$

$$\mathcal{A}_1 = \sqrt{(E'_e + m_e)(E_e - m_e)} + \sqrt{(E_e + m_e)(E'_e - m_e)}, \quad (30)$$

$$\mathcal{B}_1 = \sqrt{(E'_e + m_e)(E_e - m_e)} - \sqrt{(E_e + m_e)(E'_e - m_e)}. \quad (31)$$

In the limit ($m_e = 0$), $h = h'$ and the expression of the flux factor $\bar{\Gamma}$ coincides with Γ given in Eq. (11). Formula (20), with nonzero electron mass, is numerically included in our code for multipion electroproduction channels.

The realistic estimate of this background requires knowledge of the collimator geometry and the magnetic field configuration. This will be done by the G0 Collaboration. A quasielastic measurement on a deuterium target is also planned at TJNAF. The asymmetry term is more sensitive to the axial electric form factor G_A^e and less sensitive to the G_M^s . The π^- can be produced from the neutron in deuterium via $en \rightarrow ep\pi^-$. This channel is largely investigated in the literature.

IV. CONCLUSIONS

In this paper, we developed a model for double pion photoproduction and electroproduction on the proton, selecting diagrams which have a Δ in the intermediate state as well as those without Δ . We obtain good agreement with available photoproduction data and a reasonable agreement for the electroproduction channel, assuming a Δ in the final state. The important contribution from the D_{13} through its interference with the Kroll-Ruderman and pion pole terms is an essential ingredient in this study. It would be important to have electroproduction data where the Δ is not in the final state to check the assumptions of our model. Such measurements are planned at Graal and also at TJNAF.

The pion contamination in elastic ep scattering for the G0 experiment is manageable. On the basis of our analysis, the event generator for $ep \rightarrow ep\pi^+\pi^-$ can be constructed. Our code contains an original procedure to connect the photo- and the electroproduction of multipions without introducing the virtual photon spectrum [21]. This method is very important in the exact consideration of effects with polarized electron beams. Our event generator can be used in full detector simulations.

ACKNOWLEDGMENTS

The authors are grateful to H. Sazdjian and E. Oset for their useful discussions and to M. Mac Cormick for a careful reading of the manuscript. We would like to thank the G0 Collaboration members for constructive remarks and constant encouragements.

APPENDIX A: LAGRANGIANS

$$\mathcal{L}_{\pi NN} = -f_\pi \bar{\Psi}_N \gamma^\mu \gamma^5 \partial_\mu \vec{\phi} \cdot \vec{\tau} \Psi_N, \quad (A1)$$

$$\mathcal{L}_{\gamma NN} = -e \bar{\Psi}_N \left(F_1 \gamma^\mu A_\mu - \frac{F_2}{2M} \sigma^{\mu\nu} \partial_\nu A_\mu \right) \Psi_N, \quad (A2)$$

$$\mathcal{L}_{\pi NN\gamma} = -iq_\pi \frac{f_\pi}{m_\pi} \bar{\Psi}_N \gamma^\mu \gamma^5 A_\mu \vec{\phi} \cdot \vec{\tau} \Psi_N, \quad (A3)$$

$$\mathcal{L}_{\pi N\Delta} = \frac{g_{\pi N\Delta}}{m_\pi} \bar{\Psi}_\Delta^\mu g_{\mu\nu} (\vec{T}^+ \cdot \partial^\nu \vec{\phi}) \Psi_N + \text{H.c.}, \quad (A4)$$

$$\mathcal{L}_{\gamma N\Delta\pi} = -iq_\pi \bar{\Psi}_\Delta^\mu A_\mu (\vec{\phi} \cdot \vec{T}^+) \Psi_N + \text{H.c.}, \quad (A5)$$

$$\mathcal{L}_{\pi\pi\gamma} = ie(\phi_{[-]}\partial^\mu\phi_{[+]} - \phi_{[+]} \partial^\mu\phi_{[-]}) A_\mu, \quad (A6)$$

$$\mathcal{L}_{\gamma ND_{13}} = -\frac{G_1}{4M} \bar{\Psi}_{D_{13}}^\rho (g_{\rho\mu} \gamma_\nu - g_{\rho\nu} \gamma_\mu) \{\vec{\tau}, 1\} \Psi_N F^{\mu\nu} \\ + \frac{G_2}{8M^2} \bar{\Psi}_{D_{13}}^\rho (g_{\rho\nu} P_\mu - g_{\rho\mu} P_\nu) \{\vec{\tau}, 1\} \Psi_N F^{\mu\nu} + \text{H.c.}, \quad (A7)$$

$$\mathcal{L}_{D_{13}\Delta\pi} = i\tilde{f}_{D_{13}\Delta\pi} \bar{\Psi}_{D_{13}}^\mu g_{\mu\nu} \vec{\phi}^+ \cdot \vec{T} \Psi_\Delta^\nu \\ - i\frac{\tilde{g}_{D_{13}\Delta\pi}}{m_\pi^2} \bar{\Psi}_{D_{13}}^\mu (\partial_\mu \partial_\nu \vec{\phi}^+) \cdot \vec{T} \Psi_\Delta^\nu + \text{H.c.}, \quad (A8)$$

$$\mathcal{L}_{\pi\Delta\Delta} = -\frac{f_\Delta}{m_\pi} \bar{\Psi}_\Delta^\mu g_{\mu\nu} \gamma_\rho \partial^\nu \vec{\phi} \cdot \vec{T}_\Delta \Psi_\Delta^\rho, \quad (A9)$$

$$\mathcal{L}_{\gamma N\Delta} = -\frac{G_1}{4M} \bar{\Psi}_\Delta^\rho (g_{\rho\mu} \gamma_\nu - g_{\rho\nu} \gamma_\mu) \gamma^5 \vec{T}^+ \Psi_N F^{\mu\nu} \\ + \frac{G_2}{8M^2} \bar{\Psi}_\Delta^\rho (g_{\rho\nu} P_\mu - g_{\rho\mu} P_\nu) \gamma^5 \vec{T}^+ \Psi_N F^{\mu\nu} + \text{H.c.}, \quad (A10)$$

$$\mathcal{L}_{\gamma\Delta\Delta} = -e_\Delta \bar{\Psi}_\Delta^\sigma g_{\sigma\mu} \left(F_1^\Delta \gamma^\nu A_\nu - \frac{F_2^\Delta}{2M_\Delta} \sigma^{\nu\rho} \partial_\rho A_\nu \right) \Psi_\Delta^\mu. \quad (A11)$$

$\vec{\phi}$, Ψ_N , Ψ_Δ , $\Psi_{D_{13}}$, A_μ are the pion, nucleon, Δ , D_{13} and photon fields respectively. $\vec{\tau}$ and \vec{T}^+ are the isospin 1/2 operator and transition isospin operator from 1/2 to 3/2. For the pion fields, $\phi_{[+]}$ creates π^+ and destroys π^- and $\phi_{[-]}$ cre-

ates π^- and destroys π^+ . The four-momentum P in Eqs. (A7) and (A10) is defined as $P = p_N + p_R$ where p_N and p_R are the four-momenta of the nucleon and resonance, respectively.

In these expressions, the values of different coupling constants are $f_\pi = 1$, $g_{\pi N\Delta} = 2.06$, $G_1 = -5.57$, $G_2 = 2.97$ for the γND_{13} vertex, $\tilde{f}_{D_{13}\Delta\pi} = 0.911$, $\tilde{g}_{D_{13}\Delta\pi} = -0.552$, and $F_1^\Delta = F_1^p$, $\mu_\Delta / \mu_p = e_\Delta / e$.

APPENDIX B: FEYNMAN RULES FOR DIFFERENT VERTICES

We display in this appendix some Feynman rules in the case where the photon and the nucleon (proton) are incoming particles, while the pion π^+ is an outgoing particle:

$$V_{\pi NN} = -i\sqrt{2}f_\pi \not{p}_\pi \gamma^5, \quad (\text{B1})$$

$$V_{\gamma NN}^\mu = -e \left(F_1 \gamma^\mu + i \frac{F_2}{2M} \sigma^{\mu\nu} q_\nu \right), \quad (\text{B2})$$

$$V_{\pi NN\gamma}^\mu = -i\sqrt{2} \frac{f_\pi}{m_\pi} \gamma^\mu \gamma^5, \quad (\text{B3})$$

$$V_{\pi N\Delta}^\mu = -i \frac{1}{\sqrt{3}} \frac{g_{\pi N\Delta}}{m_\pi} p_\pi^\mu, \quad (\text{B4})$$

$$V_{\gamma N\Delta\pi} = i \frac{1}{\sqrt{3}} \frac{g_{\pi N\Delta}}{m_\pi}, \quad (\text{B5})$$

$$V_{\pi\pi\gamma}^\mu = -e(p_{\pi^+}^\mu - p_{\pi^-}^\mu), \quad (\text{B6})$$

$$V_{\gamma ND_{13}}^{\mu\nu} = -i \frac{G_1}{2M} (q^\mu \gamma^\nu - \not{q} g^{\mu\nu}) - i \frac{G_2}{4M^2} [q^\mu P^\nu - (P \cdot q) g^{\mu\nu}], \quad (\text{B7})$$

$$V_{D_{13}\Delta\pi}^{\mu\nu} = -i \frac{1}{\sqrt{3}} \left(\tilde{f}_{D_{13}\Delta\pi} g^{\mu\nu} + \frac{\tilde{g}_{D_{13}\Delta\pi}}{m_\pi^2} p_\pi^\mu p_\pi^\nu \right), \quad (\text{B8})$$

$$V_{\pi\Delta\Delta}^{\mu\nu} = i\sqrt{2} p_\pi^\mu \gamma^\nu, \quad (\text{B9})$$

$$V_{\gamma N\Delta}^{\mu\nu} = -i \frac{G_1}{2M} \sqrt{\frac{2}{3}} (q^\mu \gamma^\nu - \not{q} g^{\mu\nu}) \gamma^5 - i \frac{G_2}{4M^2} \sqrt{\frac{2}{3}} [q^\mu P^\nu - (P \cdot q) g^{\mu\nu}] \gamma^5, \quad (\text{B10})$$

$$V_{\gamma\Delta\Delta}^{\mu\rho\sigma} = -e_\Delta g_{\rho\sigma} \left(F_1^\Delta \gamma^\mu + i \frac{F_2^\Delta}{2M_\Delta} \sigma^{\mu\nu} q_\nu \right). \quad (\text{B11})$$

In order to obtain the amplitudes of various Feynman diagrams used in the model, we need an explicit expression of the propagator of the spin-3/2 resonance. For the Δ resonance, the Rarita-Schwinger propagator reads

$$G_\Delta^{\mu\nu} = \frac{\not{p} + M_\Delta}{p^2 - M_\Delta^2 + iM_\Delta \Gamma_\Delta} \left[g^{\mu\nu} - \frac{1}{3} \gamma_\mu \gamma_\nu - \frac{\gamma_\mu p_\nu - \gamma_\nu p_\mu}{3M_\Delta} - \frac{2p_\mu p_\nu}{3M_\Delta^2} \right].$$

-
- [1] D. Lücke, M. Scheunert, and P. Stichel, *Nuovo Cimento A* **58**, 234 (1968).
[2] R. Erbe *et al.*, ABBHHM Collaboration, *Phys. Rev.* **175**, 1669 (1968).
[3] J.A. Gómez Tejedor and E. Oset, *Nucl. Phys.* **A571**, 667 (1994); **A600**, 413 (1996).
[4] F. Carbonara *et al.*, *Nuovo Cimento A* **36**, 219 (1976).
[5] A. Braghieri *et al.*, *Phys. Lett. B* **363**, 46 (1995).
[6] A. Zabrodin *et al.*, *Phys. Rev. C* **55**, R1617 (1997); **60**, 055201 (1999).
[7] N.M. Kroll and M.A. Ruderman, *Phys. Rev.* **93**, 233 (1954).
[8] L.Y. Murphy and J.M. Laget, Report CEA/DAPNIA, SPhN 96-10.
[9] K. Ochi, M. Hirata, and T. Takaki, *Phys. Rev. C* **56**, 1472 (1997).
[10] V. Bernard, N. Kaiser, Ulf-G Meissner, and A. Schmidt, *Nucl. Phys.* **A580**, 475 (1994).
[11] GRAAL experiment at the ESRF, *Nucl. Phys. News* **8**, 24 (1998).
[12] J.C. Nacher and E. Oset, *Nucl. Phys.* **A674**, 205 (2000).
[13] E. Oset *et al.*, *Few-Body Syst., Suppl.* **11**, 275 (1999).
[14] S. Ong, M.P. Rekalo, and J. Van de Wiele, *Eur. Phys. J. A* **6**, 215 (1999).
[15] W. Rarita and J. Schwinger, *Phys. Rev.* **60**, 61 (1941).
[16] H. Garcilazo and E. Moya de Guerra, *Nucl. Phys.* **A562**, 521 (1993).
[17] PAC Jeopardy Proposal, The G0 Experiment (Originally E91-017)-The G0 Collaboration, 1998 (G0 Internal Report G0-98-036).
[18] H.F. Jones and M.D. Scadron, *Ann. Phys. (N.Y.)* **81**, 1 (1973).
[19] R.C.E. Devenish, T.S. Eizenschitz, and J.G. Körner, *Phys. Rev. D* **14**, 3063 (1976).
[20] K. Wacker *et al.*, *Nucl. Phys.* **B144**, 269 (1978).
[21] L. Tiator and L.E. Wright, *Nucl. Phys.* **A379**, 407 (1982); *Phys. Rev. C* **26**, 2349 (1982).